

CFD analysis of ventilation efficiency around an elevated highway using visitation frequency and purging flow rate

Hong Huang[†], Shinsuke Kato[‡], and Ryoza Ooka^{††}

Institute of Industrial Science, The University of Tokyo, 4-6-1 Komaba, Meguro-ku, Tokyo 153-8505, Japan

Taifeng Jiang^{‡‡}

Graduate School of The University of Tokyo, 4-6-1 Komaba, Meguro-ku, Tokyo 153-8505, Japan

(Received August 9 2005, Accepted June 9, 2006)

Abstract. The concentration of air pollution along roads is higher than the surrounding area because ventilation efficiency has decreased due to the high-density use of space along roads in recent years. In this study, ventilation efficiency around a heavily traffic road covered by an elevated highway and hemmed in along its side by buildings is evaluated using Visitation Frequency (VF , the frequency for pollutant to return to the objective domain) and Purging Flow Rate (PFR , the air flow rate for defining the local domain-averaged concentration). These are analyzed using Computational Fluid Dynamics (CFD) based on the standard $k-\varepsilon$ model. The VF and PFR characteristics of four objective domains are analyzed in terms of the changes in wind direction and arrangements of the fencing dividing up and down direction in the road center under the elevated highway. The resulting VFs are more than 1.0 for all cases, which means that pollutants return to the objective domain restricted by the elevated highway and side buildings. The influence of the arrangement of the buildings around the objective domain and the structure in the domain on the VF is substantial. In cases where there are no obstacles under the elevated highway, the local air exchange rate in the domain tends to be improved. Using these indices, the urban ventilation efficiencies between different urban areas can be compared easily.

Keywords: visitation frequency; purging flow rate; urban ventilation efficiency; air pollution; CFD.

1. Introduction

One characteristic of roadside air pollution in large cities is that its concentration along roads is several times higher than that of the surrounding area. This is because the vehicle emissions are trapped along the road due to the decrease in urban ventilation efficiency resulting from the high-

[†] Research Associate, Corresponding Author, E-mail: hhong@iis.u-tokyo.ac.jp

[‡] Professor

^{††} Associate Professor

^{‡‡} Graduate Student

density use of space, such as high-rise buildings in urban areas and multi-layered roadways. In order to alleviate air pollution at the urban planning stage, it is important to improve the effectiveness of air pollution removal; in other words, reduce the average concentration in the local domain and improve the ventilation efficiency of the local area, including pedestrian zones or roadside areas. Improving the urban ventilation becomes the common interest of both urban planners and urban climatologists (WMO 1996).

Research works have been done on the evaluation and improvement of urban ventilation. These works may come from field measurements, fluid dynamics experiments with wind tunnels, water tanks and water tunnels (Hunt, *et al.* 1976, Peterka 1983). In recent years, the revolutionary progress in numerical modeling and radical improvements in computational capacity, the application of CFD (Computational Fluid Dynamics) technique began to play an important role in the evaluation of the urban ventilation (Boggs, *et al.* 1989, Mochida, *et al.* 1992, Nicholls, *et al.* 1995, Liu, *et al.* 2002, Fang, *et al.* 2004). However, they all just focused on simulating the wind environment or pollutant dispersion around some buildings, no standard or indices for evaluating the urban ventilation efficiency were suggested. The urban ventilation efficiencies between different urban areas, which have different structures, can be compared easily using some standard or indices, which is very useful for urban planning and urban environment improvement.

On the other hand, the ventilation efficiency of the local domain within an indoor area, that is, the mechanism of the local domain-averaged concentration, is analyzed by the ventilation efficiency indices, visitation frequency, purging flow rate and the average staying time in the local domain (Sandberg, *et al.* 1992, Ito, *et al.* 2000, Kato, *et al.* 2003). It is thought that these ventilation efficiency indices are also effective in evaluation of the effectiveness of air pollution removal by the wind in outdoor areas, which is to say, the ventilation efficiency in the urban area. Thus it is possible to clarify the relationship between the structure of the local domain with the exhaust characteristic of the pollutants generated or flowing in the local domain, which demonstrates the benefits of conducting air pollution improvement plan. In this study, the ventilation efficiency around a heavily traffic road, where the pollutant concentration is high, is evaluated using Visitation Frequency (VF), Purging Flow Rate (PFR) and the average staying time (T_p), and the air pollution structure of the local domain which includes an elevated highway and many buildings alongside the road is clarified. The effectiveness of VF and PFR for evaluating the urban ventilation efficiency is confirmed.

2. Ventilation efficient indices

2.1. Definition of local domain

As the pollutant concentration in urban areas is not uniform, it is important to evaluate the average concentration of the pollutant in the local domain. In this paper, 'local domain' is introduced to represent a partial zone in whole urban space, such as pedestrian zone or an occupied zone. The purpose of this research is to analyze how the local domain-averaged concentration is determined by VF and T_p .

2.2. Visitation frequency

An uneven distribution of pollutant concentration occurs in urban areas. This is because wind flow has direction, obstacles exist, the pollutant source is not constant, and so on. In this study, in

order to evaluate not only the level of the uneven pollutant concentration, but also the pollutant behavior including how much returns, circulates and stays in the local domain, what determines the pollutant concentration in the local domain, the VF and T_p are introduced. VF means the average frequency with which pollutants generated in the local domain return to the local domain after once being transported outside it. $VF = 1$ means that after being generated, the pollutant stays only once in the local domain, and after leaving the local domain, it never returns. $VF = 2$ means that the pollutant first stays in the local domain, is transported outside, and then returns to the local domain where it stays once again due to the re-circulating flow. This is an important parameter that shows the smoothness of the exhaust of such pollutants generated or the flow into the local domain. VF can be obtained from the calculation of a particle tracking method based on Large Eddy Simulation (LES), or calculation of the passive pollutant flux method based on Reynolds Averaged Navier-Stokes equation (RANS). VF is defined as:

$$VF = 1 + (J_p/M_p) = 1 + (\Delta q_p/q_p) \quad (1)$$

where J_p is the amount of particles, visiting (returning to) the local domain 'P' per unit time (particle/sec); M_p is the amount of particles generated in the local domain (particle/sec); Δq_p is the inflow (returning) flux of pollutant into the local domain 'P' per unit time (kg/sec); and q_p is the pollutant generation rate per unit time (kg/sec).

2.3. Average staying time

The average staying time represents the average time that the pollutant takes from once arriving into or being generated in the local domain to its leaving. Multiplying T_p by VF indicates the total average staying time (lifespan of the pollutant) in the local domain. It is possible to evaluate the structure of the average concentration in the local domain by evaluating VF and T_p at the same time.

2.4. Purging flow rate

Purging flow rate is the effective airflow rate required to remove/purge the pollutant from the local domain, which in effect shows the removal efficiency of the pollutant. It has a close relation with VF , which shows the characteristic of concentration distribution and pollutant removal. PFR , which is defined as the net ventilation rate of the local domain by the pollutant generation rate and the average concentration, can also be defined by the VF and the average staying time:

$$PFR = q_p/C_p = V_p/(VF \times T_p) \quad (2)$$

where V_p is the volume of the local domain (m^3), C_p is the local domain-averaged concentration (kg/m^3). It can be seen that PFR is the effective ventilation rate of the local domain.

In this research, these indices are applied to the air pollution of an urban area around an elevated highway, and the ventilation efficiency of the local domain is examined.

3. CFD simulation

Detailed VF information can be obtained using Lagrange tracking (the middle of the Eq. (1)) of particles flowing in or out of the local domain. However, it is convenient to calculate VF from the average characteristic of the flow field in the case that the interest is in the average behavior. This has

been shown to be effective in analyzing *VF* and *PFR* using the average pollutant distribution simulation by the RANS model (Davidson and Olsson 1998), which is based on the ensemble average. In this study, the standard $k-\varepsilon$ model (Launder and Spalding 1974) are used for CFD analysis.

3.1. CFD model description

Air flow in urban environment issue is generally assumed to be three-dimensional and incompressible. As is already well known, the cornerstone of industrial CFD is the Navier-Stokes (NS) equation set, expressed for turbulent flows in terms of suitably-averaged velocities and pressures to make them amenable to numerical solution without excessive computing overheads. The conventional

Table 1 Governing equations

Continuity equation

$$\frac{\partial \langle u_i \rangle}{\partial x_i} = 0 \quad (3)$$

Momentum equation

$$\frac{\partial \langle u_i \rangle}{\partial t} + \frac{\partial \langle u_i \rangle \langle u_j \rangle}{\partial x_j} = -\frac{1}{\rho} \frac{\partial \langle p \rangle}{\partial x_i} + \frac{\partial}{\partial x_j} \left(\nu \left(\frac{\partial \langle u_i \rangle}{\partial x_j} + \frac{\partial \langle u_j \rangle}{\partial x_i} \right) - \langle u'_i u'_j \rangle \right) \quad (4)$$

Species transport equation

$$\frac{\partial \langle C_i \rangle}{\partial t} + \frac{\partial \langle u_i \rangle \langle C_i \rangle}{\partial x_i} = \frac{\partial}{\partial x_i} \left(D \frac{\partial \langle C_i \rangle}{\partial x_i} - \langle u'_i C_i \rangle \right) \quad (5)$$

Turbulent energy transport equation

$$\frac{\partial k}{\partial t} + \frac{\partial \langle u_j \rangle k}{\partial x_j} = P_k + D_k - \varepsilon \quad (6)$$

Turbulent dissipation rate equation

$$\frac{\partial \varepsilon}{\partial t} + \frac{\partial \langle u_j \rangle \varepsilon}{\partial x_j} = D_\varepsilon + \frac{\varepsilon}{k} (C_{\varepsilon 1} P_k - C_{\varepsilon 2} \varepsilon) \quad (7)$$

$$-\langle u'_i u'_j \rangle = \nu_t \left(\frac{\partial \langle u_i \rangle}{\partial x_j} + \frac{\partial \langle u_j \rangle}{\partial x_i} \right) - \frac{2}{3} k \delta_{ij} \quad (8) \quad \nu_t = C_\mu \frac{k^2}{\varepsilon} \quad (9)$$

$$-\langle u'_i C_i \rangle = \frac{\nu_t}{\sigma_w} \frac{\partial \langle C_i \rangle}{\partial x_i} \quad (10) \quad P_k = -\langle u'_i u'_j \rangle \frac{\partial \langle u_i \rangle}{\partial x_j} \quad (11)$$

$$D_k = \frac{\partial}{\partial x_j} \left(\frac{\nu_t}{\sigma_k} \frac{\partial k}{\partial x_j} \right) \quad (12) \quad D_\varepsilon = \frac{\partial}{\partial x_j} \left(\frac{\nu_t}{\sigma_\varepsilon} \frac{\partial \varepsilon}{\partial x_j} \right) \quad (13)$$

$$\sigma_k = 1.0, \quad \sigma_\varepsilon = 1.3, \quad \sigma_w = 0.9, \quad C_{\varepsilon 1} = 1.44, \quad C_{\varepsilon 2} = 1.92$$

and still most widely-used approach is time averaging, also described as Reynolds averaging, in which the NS equations are transformed as the Reynolds-Averaged Navier-Stokes (RANS) set. Moreover, the approach of the standard $k-\varepsilon$ model (Launder and Spalding 1974), which is widely and practically useful, is adopted for solutions. The equations governing the mass and momentum transportation of wind flow are shown as Eqs. (3)~(13) in Table 1. where k , ε presents the turbulence kinetic energy and dissipation rate; and C_{μ} , σ_k , σ_{ε} , $C_{\varepsilon 1}$, $C_{\varepsilon 2}$ are model constants.

Although the standard $k-\varepsilon$ model shows some problem in the prediction of the wake phenomenon around buildings, such as the overestimate of turbulent kinetic energy around windward corner (Murakami, *et al.* 1988), it stills has a good reputation for reliability in the field of wind engineering (Murakami 1990) and air pollutant diffusion analysis (Huang, *et al.* 2000).

3.2. CFD model validation

3.2.1. Analysis object

Validation of the CFD model is examined by comparing the numerical simulation with a field measurement data. The field measurement was carried out on 2nd February, 2005 by measuring the concentrations of NO at the integral points from 10:00 to 15:00 near the Ikegami-Shinmachi crossing in Kawasaki City, Japan, as shown in Fig. 1. There is a southwest-northeast direction elevated highway - the Capital Highway - and a main local road underneath the highway. Kawasaki city is between Yokohama and Tokyo city, in the Kanto region of Japan. It is well known as being a center for heavy industry and has been developed as an extent urbanized region. The buildings here are of various geometrical configurations and functions, such as residential houses, commercial offices, shopping centers, heavy industrial facilities. All of these building blocks are seemingly integrated to form a big congregation. Intensive human and industrial activities in this area generate heavy transportation load and raise the concern of air pollution induced by traffic road. In addition, house colony with excessive density narrow the width of street canyons and give negative effect on pollutants dispersion more or less. There are also several pieces of fence installed under part of the elevated highway. These fences are dense plants. There is almost no permeability. Therefore, the fence is assumed to be solid wall here

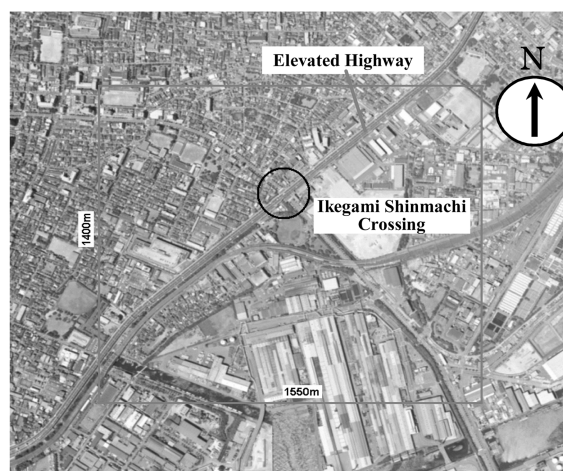


Fig. 1 Analysis object

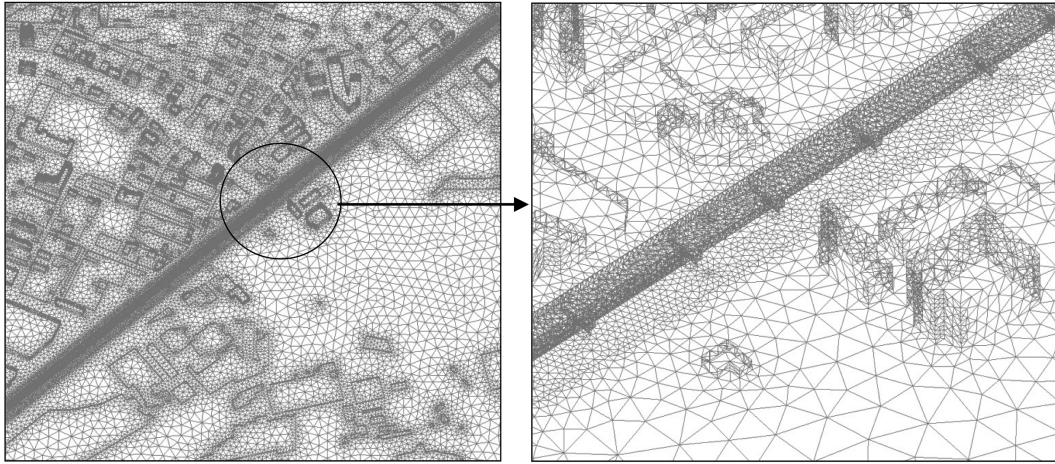


Fig. 2 A part of the unstructured computational grid

(We can see that it is reasonable from the later comparative study).

3.2.2. Computational grid

The urban area is very complex here because there are local roads, highways and many buildings, as well as fences under some parts of the elevated highway. The use of an unstructured computational grid is effective for conducting a CFD simulation in such a complex urban area (Huang, *et al.* 2005). An unstructured grid of 1,830,000 meshes was made based on the geographical data provided by the Ministry of Land, Infrastructure and Transport. The minimum resolution of the grid is 1.0 m around the highway. Fig. 2 shows a part of the finished unstructured computational grid for the analysis area.

3.2.3. Simulation conditions

The solution of the governing equations is solved by the finite-volume method using Star-CD software. A staggered grid system is employed for the vector (U_i) and scalar (P , C , k , ϵ) units. A hybrid second-order scheme named MARS (Monotone Advection and Reconstruction Scheme) (STAR-CD 2001) is applied to the convective terms. Conservation of mass is obtained by using the SIMPLE pressure correction algorithm (Patankar 1980). Table 2 shows details of the analysis conditions. The inflow wind velocity is set at $1/4^{\text{th}}$ power profile. The representative length Z_0 was based on the height of the meteorological observation station provided by the Kawasaki City pollution control center. A constant flux layer was assumed for the turbulent energy k , and turbulent intensity was assumed to be 10% of the inflow velocity of the wind at a representative height (Z_0) of 16 meters.

It was known that hardly any of the pollutants emitted from the vehicles on the elevated highway would reach pedestrian level from a wind tunnel experiment (Takahashi, *et al.* 2004), and thus only the ground level local road in the southwest-northeast direction was considered as an exhaust source. The measurement data at 11:00 was used for the validation. The meteorological conditions and pollutants emission intensity are listed out in Table 3. The temperature in the sky is 6.9°C which is the Automated Meteorological Data Acquisition System (AMeDAS) data of Japan Meteorological Agency. The ground temperature is estimated to be about 7.0°C at the beginning of

Table 2 Analysis conditions

Turbulent model	Standard $k - \varepsilon$ model
Differential scheme	Convection terms: MARS*
Inlet	$U = U_0 \cdot (Z/Z_0)^{1/4}, Z_0 = 16m$
	$k = 1.5 \cdot (I \times U)^2, I = 0.1$
	$\varepsilon = C_\mu \cdot k^{3/2} / l$
	$l = 4(C_\mu \cdot k)^{1/2} Z_0^{1/4} Z^{3/4} / U_0$ (Murakami, et al. 1988)
Side, sky	Free slip
Wall	Generalized logarithmic law

*MARS: Monotone Advection and Reconstruction Scheme, second-order scheme (STAR-CD 2001)

Table 3 Meteorological condition and pollutant emission intensity

Meteorological condition		Emission rate of NO (g/m ³ h)	
U_0 ($Z_0=16m$) (m/s)	Wind direction	UP* ¹	DOWN* ²
3.7	W	1.41	1.16

*1 Towards Tokyo City (Northeast)

*2 Towards Yokohama City (Southwest)

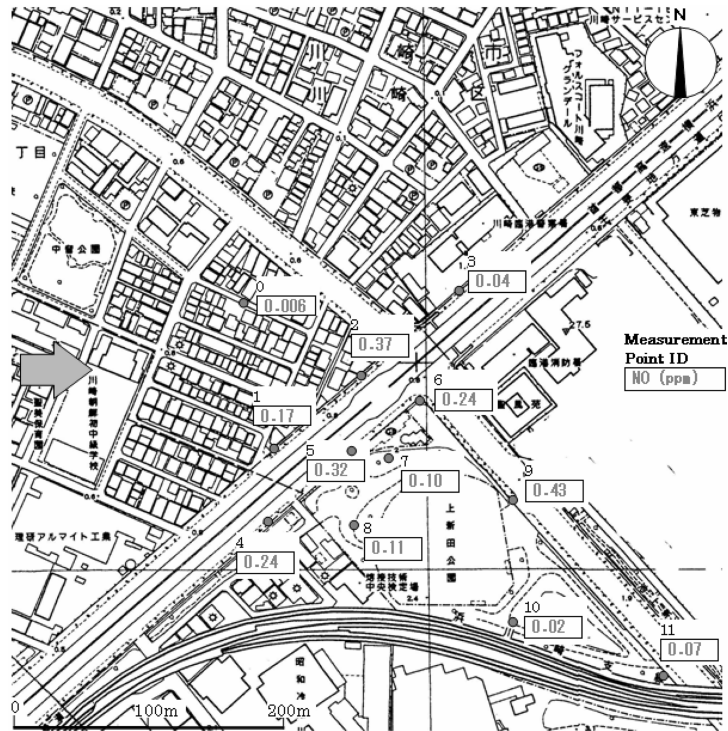


Fig. 3 NO concentration at each point at 11:00 of the field measurement

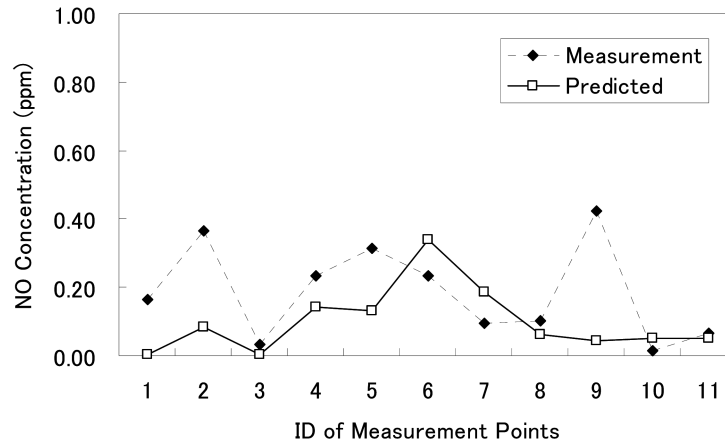


Fig. 4 Comparison between the CFD simulation results and the field measurement data

Feb (Hwang, *et al.* 2005). Therefore, an isothermal condition is used here.

3.2.4. Validation

Fig. 3 shows the NO concentration at each point at 11:00 of the field measurement. During the measurement process, not only were the southwest-northeast oriented roads the emission sources, but pollutant exhaust also include numerous other components, such as roads in other directions. Therefore, it is appropriate to consider the measurement results of the concentration in the upstream area as the background concentration. Here, the background value is 0.006 ppm (point 0 in Fig. 3) for NO.

The comparison between the CFD simulation results and the field measurement data is presented in Fig. 4. Good agreement can be recognized from the comparative results. A higher concentration in the measurement data than the simulation result can be observed at points 2 and 9. This is because that points 2 and 9 are both very close to another local road. The road lies within the objective domain running in SE-NW direction, which was not set as a pollutant source in the calculation. The accuracy is considered to be acceptable enough for the simulation of so much complex urban area.

4. Outline of calculation of *VF* and *PFR*

VF and *PFR* were calculated over the same urban area as the validation of the CFD in order to evaluate the ventilation efficiency around the elevated highway.

4.1. Local domain setting and calculation cases

In order to study the ventilation efficiency around the elevated highway, four local domains, as shown in Figs. 5 and 6 are set. Volume 1 (1500 m(L) × 36 m(W) × 16 m(H)) includes all of the elevated highway and the main local road in the analysis object. Volume 2 (300 m(L) × 36 m(W) × 16 m(H)) is the domain where the fencing under the elevated highway is low (about 2.5 meters high), Volume 3 (300 m(L) × 36 m(W) × 16 m(H)) is the domain where the fencing is high (about 7.5 meters high), while Volume 4 (60 m(L) × 36 m(W) × 16 m(H)) is the domain around the crossing.

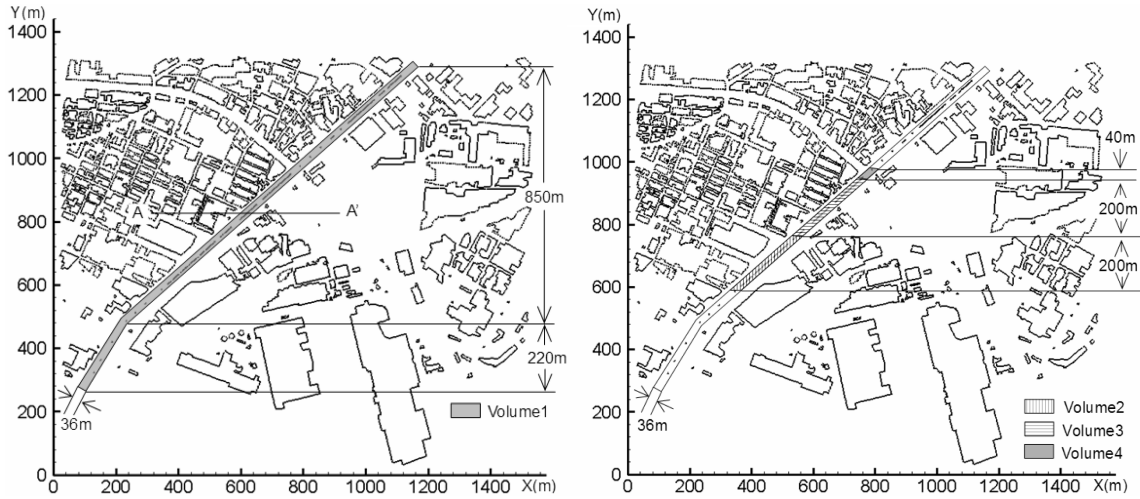


Fig. 5 Local domain for analysis (Horizontal plane)

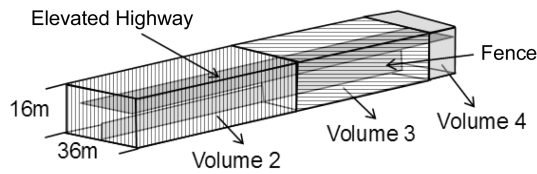


Fig. 6 Image of the local domain

Table 4 Analysis cases

	Wind direction	Wind velocity	With fencing or not
Case 1	SE	1.9 m/s	With
Case 2	NW	1.9 m/s	With
Case 3	SE	1.9 m/s	Without

Moreover, three cases were conducted, as shown in Table 4. The used inflow wind velocity which is an AMeDAS data is fixed, while the direction is changed. In this study, the objective is to propose and confirm the effectiveness of VF and PFR for evaluating the urban ventilation efficiency. An isothermal condition is also used here, which is the same as the condition in the validation.

4.2. Calculation of VF and PFR

In order to obtain VF , PFR , and T_p , the pollutant diffusion analysis was conducted as the following process. First, the flow field was analyzed. Second, the concentration field where the pollutant, which is assumed to be a Passive Pollutant was generated uniformly throughout the local domain was analyzed, and the flow field analyzed before was fixed here. Then the VF was obtained by calculating inflow flux to the local domain based on the average pollutant diffusion analysis. Moreover, the PFR was obtained from the average concentration of the local domain. T_p was obtained by the Eq. (2).

5. Results and discussion

5.1. Average wind distribution

Figs. 7, 8 and 9 show the simulation results of the horizontal wind velocity scalar distribution at a height of 1.5 meters in the whole analysis area for Cases 1, 2 and 3 respectively. The wind velocity is about 1.2~1.6 m/s in the area on the southeast side of the elevated highway, and is seen to

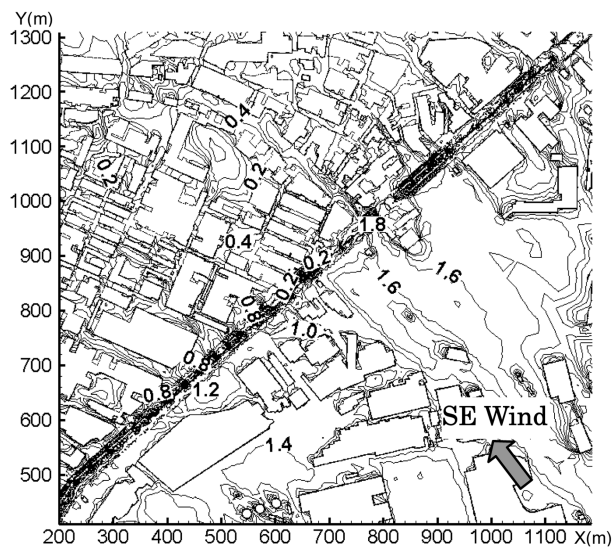


Fig. 7 Horizontal wind velocity scalar distribution in the whole area (Case 1, height: 1.5 m)

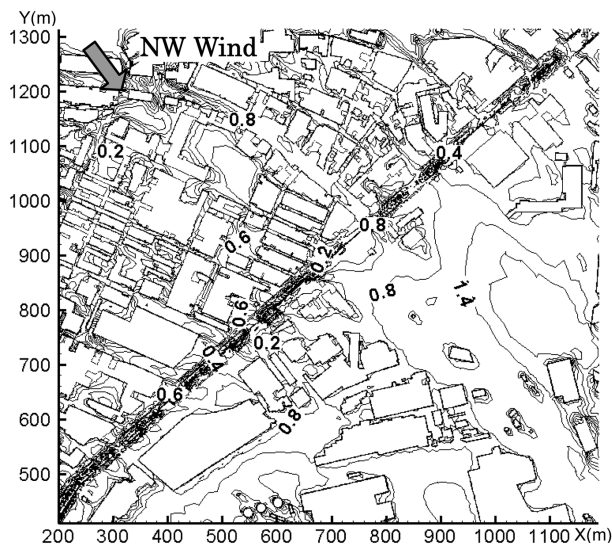


Fig. 8 Horizontal wind velocity scalar distribution in the whole area (Case 2, height: 1.5 m)

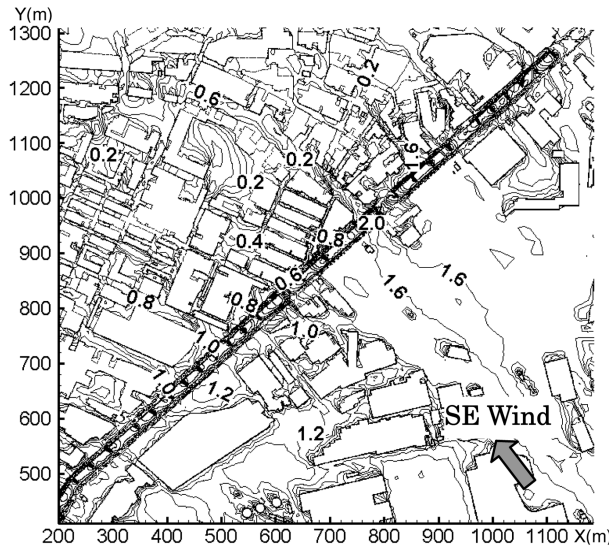


Fig. 9 Horizontal wind velocity scalar distribution in the whole area (Case 3, height: 1.5 m)

decrease to about 0.2~0.8 m/s on the northwest side where the building density is higher than on the southeast side in Case 1 and 3. When there is fencing (Case 1), the velocity of the wind in Volume 2 (refer to Figs. 5 and 6), which features low fencing, is about 0.8 m/s; whereas in Volume 3 (refer to Figs. 5 and 6), which has high fencing, it decreases to 0.2 m/s, thus forming a static region for pollutants under the elevated highway. When there is no fencing (Case 3), the wind passes smoothly under the elevated highway at about 0.8~1.0 m/s, and the wind also flows smoothly at the crossing because there are no obstacles. For Case 2, the inflow wind direction is northwest, and the velocity of the wind under the elevated highway is lower than that of Case 1 because the density of the buildings on the windward side of the elevated highway is a little higher. Figs. 10, 11, and 12 show

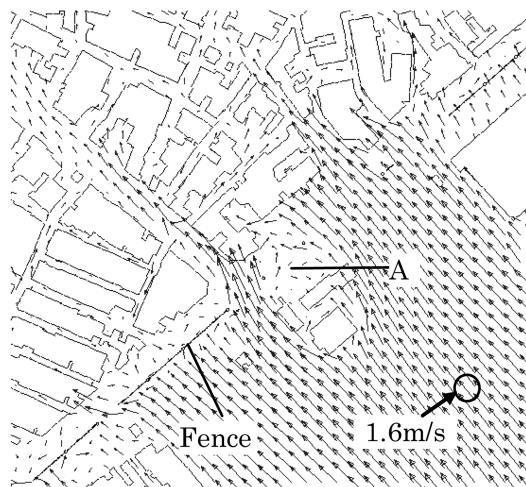


Fig. 10 Horizontal wind velocity vector distribution around the crossing (Case 1, height: 1.5 m)

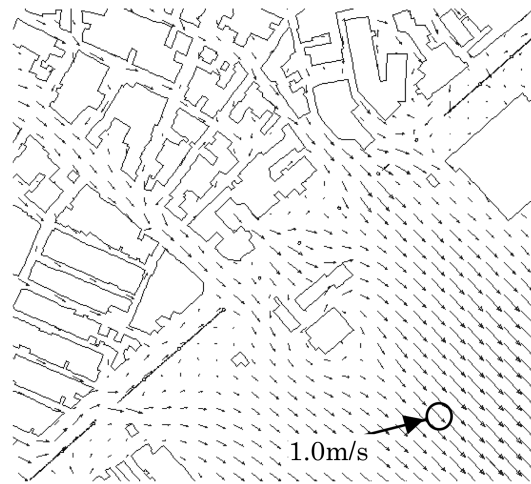


Fig. 11 Horizontal wind velocity vector distribution around the crossing (Case 2, height: 1.5 m)

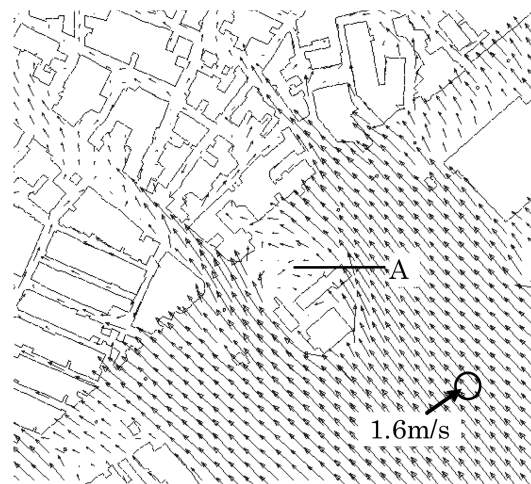


Fig. 12 Horizontal wind velocity vector distribution around the crossing (Case 3, height: 1.5 m)

the simulation results of the horizontal wind velocity vector distribution of at a height of 1.5 meters around Ikekagmi-Shinmachi crossing for Cases 1, 2, and 3 respectively. It can be seen that the wind is weaker behind the fences if fences exist, and circulatory flow occurs between the fences and the buildings. To the right of the crossing (Area A in Figs. 10 and 12) in Case 1 and 3, a vortex is formed behind the buildings.

5.2. The results of average pollutant diffusion analysis

The resulting VF , T_p , PFR , and C_p are shown in Table 5 based on average pollutant diffusion analysis results. Moreover, T_p , PFR , and C_p are normalized to the results of Volume 1 in Case 1. Fig. 13 shows C_p (the local domain-average concentration). Fig. 14 shows the relationship between

Table 5 Results of VF , PFR , and T_p

Case 1				
	Vol. 1	Vol. 2	Vol. 3	Vol. 4
VF	1.11	1.06	1.28	1.24
T_p	1.00	0.80	1.86	1.27
PFR	1.00	0.26	0.09	0.03
C_p	1.00	0.77	2.15	1.42
Case 2				
	Vol. 1	Vol. 2	Vol. 3	Vol. 4
VF	1.13	1.14	1.25	1.17
T_p	1.21	0.99	2.03	1.14
PFR	0.82	0.20	0.08	0.03
C_p	1.23	1.01	2.28	1.20
Case 3				
	Vol. 1	Vol. 2	Vol. 3	Vol. 4
VF	1.06	1.07	1.06	1.18
T_p	0.67	0.64	0.69	0.59
PFR	1.54	0.32	0.30	0.06
C_p	0.65	0.62	0.65	0.63

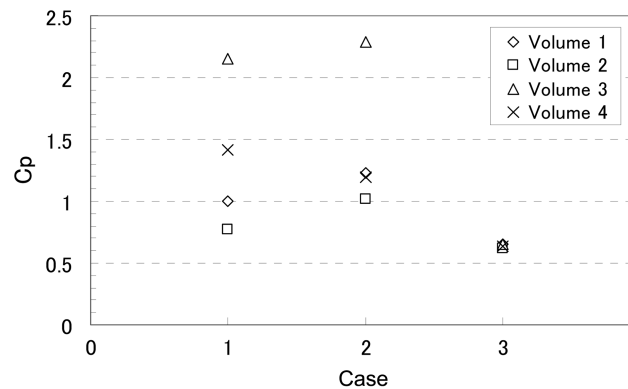
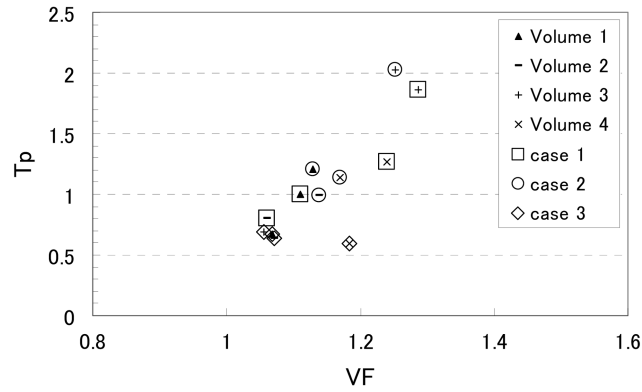
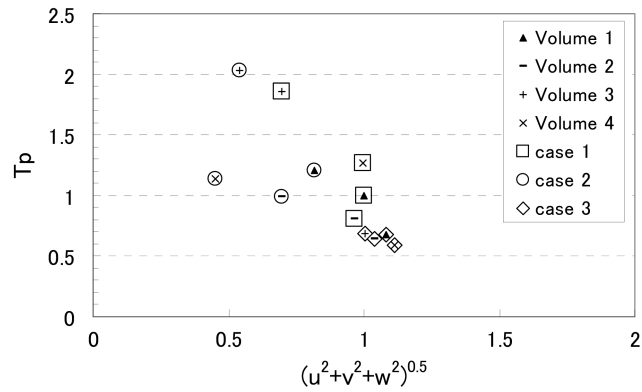


Fig. 13 Local domain-averaged concentration

VF and T_p . Fig. 15 shows the relationship between the wind velocity scalar and T_p . Figs. 16 and 17 show the velocity of the wind distribution and the concentration distribution in section A-A' (see Fig. 5).

5.2.1. Distribution of C_p

As shown in Fig. 13, when there is fencing (Cases 1 and 2), the C_p of Volume 3 (the domain

Fig. 14 Relationship between VF and T_p Fig. 15 Relationship between the wind velocity scalar and T_p

where the fencing is high) is higher than that of Volume 2 (the domain where the fencing is low). It is thought that the pollutant is rendered static due to the weak wind velocity and the circulatory flow between the buildings and the fencing on both sides of the elevated highway, as shown in Figs. 16 and 17. The C_p in Case 2 tends to be a little higher than that of Case 1 because the inflow direction is northwest and the velocity of the wind under the elevated highway is lower than in Case 1, as has been described in the section 4.1. When there is no fencing (Case 3), the ventilation situation under the elevated highway looks similar, and the C_p in each Volume hardly changes. It is considered that the arrangement of the fencing has significant influence on the average concentration distribution of pollutants in the local domain.

5.2.2. Distribution of VF and T_p

VF is the value of more than 1.0 for all cases as shown in Table 5 and Fig. 14. This indicates that the return or circulation of pollutants is confirmed in the local domain around the elevated highway. In Case 1, the VF of Volumes 3 and 4 is high. This is thought to indicate that a circulatory flow occurs between the fences and the buildings due to the high fencing in the local domain. The T_p is also large for the same reason. The velocity of the wind around the elevated highway tends to be

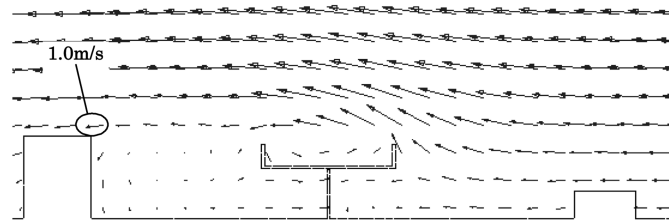


Fig. 16 Wind distribution of section A-A'

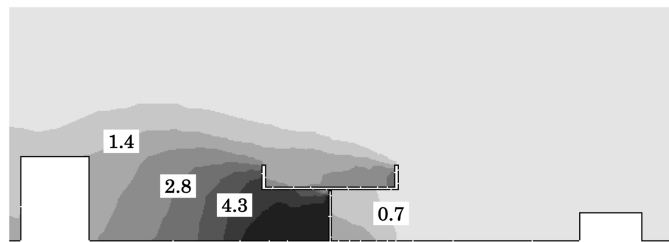


Fig. 17 Concentration distribution of section A-A' (Normalized to the averaged concentration)

lower in Case 2 because of the wind from the northwest (see the previous section 4.1), and the T_p becomes longer. As there is no fence in Case 3, little pollutant is circulated or returned, and each local domain exhibits almost the same value for VF and T_p except for Volume 4. It is thought that the degree of influence on the ventilation conditions of the local domain under the elevated highway was the same because the overall heights of the buildings are low and almost uniform in this analysis area. The larger VF of Volume 4 is because a vortex is formed at the right side of the crossing (see Fig. 14), which increases the amount returned. It can be concluded that the arrangement of the buildings and the structure in the local domain have a large influence on VF . T_p tends to increase in line with an increase in VF as shown in Fig. 14. This is thought to be the reason for the high C_p value. As shown in Fig. 15, T_p is in inverse proportion to the average velocity of the wind in the local domain, T_p becomes shorter as the average velocity of the wind increases.

5.2.3. Distribution of PFR

The PFR is the effective ventilation rate, which means how much fresh air is supplied in the local domain. PFR depends on the size of the local domain, and if it is small, the PFR becomes small. In order to easily compare one against the other, the air exchange rate is used here. The air exchange rate of the local domain is obtained by dividing PFR by the volume of the local domain. Fig. 18 shows the air exchange rate of each local domain (normalized to the result of Volume 1 for Case 1). The air exchange rate of the local domain for Volume 3, where the fencing is high, decreases compared with that of Volume 2, where the fencing is low. When there is no fencing (Case 3), the air exchange rate of the local domain tends to rise. This means the urban ventilation efficiency of this case is better than those of others. Moreover, the C_p of Case 3 is almost the same due to the same air exchange rate for each Volume.

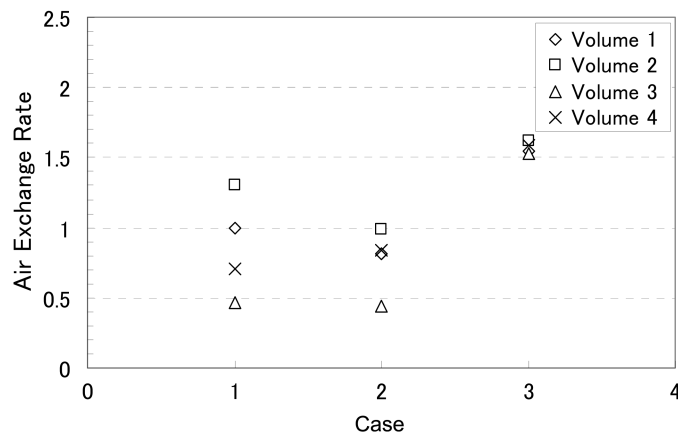


Fig. 18 Air exchange rate distribution (Normalized to Case 1)

6. Conclusions

In this study, the ventilation characteristic around an elevated highway where there is thought to be high concentration of air pollutants was evaluated using visitation frequency, purging flow rate and the average staying time. The air pollution structure of the local domain was analyzed using CFD based on average diffusion analysis. The conditions, including wind direction, obstacle positions and so on, were changed, and then the VF , T_p , and PFR were examined. The resulting VF s are shown to be more than 1.0 in all cases, which indicates that pollutants return or circulate within the objective domain including the elevated highway and hemmed in by buildings along the side. The influence on the VF of the arrangement of the buildings around the objective domain and structures in the domain is large. In the case where there are no obstacles under the elevated highway, the air exchange rate tends to be improved. Using these indices, the urban ventilation efficiencies between different urban areas can be compared easily. It can give value suggestion on the urban planning and urban environment improvement, including the arrangement and shapes of buildings, highways even trees and so on.

References

- Boggs, D. W. and Peterka, J. A. (1989), "Aerodynamic model tests of tall buildings", *J. Eng. Mech.*, **115**, 618-635.
- Davidson, L. and Olsson, E. (1998), "Calculation of age and local purging flow rate in rooms", *Building and Environ.*, **22**, 111-127.
- Fang, X., Jiang, W., Miao, S., Zhang, N., Xu, M., Ji, C., Chen, X., Wei, J., Wang, Z., and Wang, X. (2004), "The multi-scale numerical modeling system for research on the relationship between urban planning and meteorological environment", *Advances in Atmospheric Science*, **21**, 1, 103-112.
- Huang, H., Akutsu, Y., Arai, M., and Tamura, M. (2000), "A two-dimensional air quality model in an urban street canyon: Evaluation and sensitivity analysis", *Atmospheric Environ.*, **34**, 689-698.
- Huang, H., Ooka, R., and Kato, S. (2005), "Urban thermal environment measurements and numerical simulation for an actual complex urban area covering a large district heating and cooling system in summer", *Atmospheric Environ.*, **39**, 6362-6375.

- Hunt, J. C. R., Poulton, E. C., and Mumford, A. (1976), "The effect of wind on people: New criteria based on wind tunnel experiment", *Building and Environ.*, **2**, 15-28.
- Hwang, S., Ooka, R., Nam, Y., and Sekine, K. (2005), "The development of geothermal air-conditioning system using ground heat exchange utilizing building's cast-in-place concrete pile foundation (Part 9), development of simulation models base on numerical simulation of soil heat transfer", *Summaries of Technical Papers of Annual Meeting of Architectural Institute of Japan*, **D2**, 667-668 (in Japanese).
- Ito, K., Kato, S., and Murakami, S. (2000), "Study of visitation frequency and purging flow rate based on averaged contaminant distribution, study on evaluation of ventilation effectiveness of occupied space in room", *J. Archit. Plann. Environ. Eng., AIJ*, **529**, 31-37 (in Japanese).
- Kato, S., Ito, K., and Murakami, S. (2003), "Analysis of visitation frequency through particle tracking method based on LES and model experiment", *Indoor Air*, **13**, 182-193.
- Lauder, B. E. and Spalding, D. B. (1974), "The numerical computation of turbulent flows", *Comp. Mech. Eng.*, **3**, 269-289.
- Liu, H., Sang, J., Zhang, B., Chan, J. C. L., Cheng, A. Y. S., and Liu, H. (2002), "Influences of structures on urban ventilation: A numerical experiment", *Advances in Atmospheric Science*, **19**, 6, 1045-1054.
- Mochida, A., Murakami, S., and Shoji, M. (1992), "Numerical simulation of flow field around texas tech building by large eddy simulation", *First International Symposium on Computational Wind Engineering*, 16-34.
- Murakami, S. (1990), "Numerical simulation of turbulent flow field around cubic model current status and applications of $k-\epsilon$ model and LES", *J. Wind Eng. Ind. Aerodyn.*, **33**, 139-152.
- Murakami, S. Mochida, A., and Hayashi, Y. (1988), "Modification of production terms in $k-\epsilon$ model to remove overestimate of k value around windward corner", *10th Wind Engineering Symposium*, 199-204 (in Japanese).
- Nicholls, M. E., Peilke, R. A., and Eastman, J. L. (1995), "Applications of RANS numerical model to dispersion over urban areas", *Wind Climate in Cities*, Kluwer Academic Publisher, 703-732.
- Patankar, S. V. (1980), *Numerical Heat Transfer and Fluid Flow*, McGraw-Hill, New York.
- Peterka, J. A. (1983), "Selection of local peak pressure coefficients for wind-tunnel studies of buildings", *J. Wind Eng. Ind. Aerodyn.*, **13**, 477-488.
- Sandberg, M. (1992), "Ventilation effectiveness and purging flow rate - A review", *International Symposium on Room Air Convection and Ventilation Effectiveness*, 1-21.
- STAR-CD, (2001), "Methodology, STAR-CD Version 3.15", Computational Dynamics Limited.
- Takahashi, T., Kato, S., Ooka, R., Kouno, R., and Watanabe, T. (2004), "Study on prediction of pollutant dispersion on urban area (Part 1), wind tunnel study on contaminant diffusion of traffic on existing urban area", *Summaries of Technical Papers of Annual Meeting of Architectural Institute of Japan*, **D2**, 815-816 (in Japanese).
- World Meteorological Organization (1996), "Climate and urban development", WMO-No. 844, 256.